We are IntechOpen,
the world's leading publisher of
Open Access books
Built by scientists, for scientists

6,900
Open access books available

185,000
International authors and editors

200M
Downloads

154
Countries delivered to

Our authors are among the

TOP 1%
most cited scientists

12.2%
Contributors from top 500 universities

BOOK CITATION INDEX
CLARIVATE ANALYTICS
INDEXED

WEB OF SCIENCE™

Selection of our books indexed in the Book Citation Index
in Web of Science™ Core Collection (BKCI)

Interested in publishing with us?
Contact book.department@intechopen.com

Numbers displayed above are based on latest data collected.
For more information visit www.intechopen.com

Reliability of Microelectromechanical Systems Devices

Wu Zhou, Jiangbo He, Peng Peng, Lili Chen and Kaicong Cao

Abstract

Microelectromechanical systems (MEMS) reliability issues, apart from traditional failure mechanisms like fatigue, wear, creep, and contamination, often involve many other specific mechanisms which do not damage the system's function but may degrade the performance of MEMS devices. This chapter focuses on the underlying mechanisms of specific reliability issues, storage long-term drift and thermal drift. The comb finger capacitive micro-accelerometers are selected as the case for this study. The material viscoelasticity of packaging adhesive and thermal effects induced by structure layout are considered so as to explain the physical phenomenon of output change over time and temperature. Each section showcases the corresponding experiments and analysis of reliability.

1. Introduction

Microelectromechanical systems technology has been widely applied in areas such as inertial navigation, RF/microwave communications, optical communications, energy resources, biomedical engineering, environmental protection, and so on. The MEMS-related products involve micro-accelerometers, gyroscopes, micro-resonators, microswitches, micro-pumps, pressure sensors, energy harvesters, etc. Many new designs and prototypes of MEMS are produced and marketed in large numbers year by year. Only a few, however, can be used as mature products in the field with requirements for high performance. The main obstacle is that the reliability issues of micro systems involve numerous physical failure mechanisms covering the aspects of mechanical structures, electrical components, and packaging and working conditions [1–6].

The industrial standards for MEMS reliability, so far, are not existent because the behavior of MEMS is highly dependent on the designs and fabrication of specific micro systems. This is attributed to the complication and diversity of micro-devices. The coupling effects between different physical domains add much more complexities to the analysis of failure modes. For example, the effects of thermal expansion are not only determined by the difference of coefficients of thermal expansion (CTE) but are equally highly impacted by the structural layout [7, 8]. A failure mode, therefore, can exhibit many different reliability phenomena in different

devices; meanwhile, the exhibited same phenomenon like drift and stability may not result from the same physical mechanism. Current publications on MEMS' reliability involved almost every aspect of micro systems including structures, electrical components, materials, electronics, packaging, and so on. Performed literature research reveals a wide coverage of topics, ranging from basic physical mechanisms to engineering applications and from single structural units to entire device systems. Compared with the failure modes of mechanical structures and electrical components which have a certain similarity to macro systems [9–17], the reliability issue of systematical behaviors is significantly more important because it always originates from the interaction between its components or sub-systems which by themselves can work normally [18–20].

In this chapter, the typical reliability issue regarding the MEMS packaging effects of micro-accelerometer, selected as a specific device, is concerned. MEMS packaging, developed from integrated circuit (IC) packaging, is to integrate the fabricated device and circuit. Yet, the two packaging technologies are significantly different. The functions of IC packaging are mainly to protect, power, and cool the microelectronic chips or components and provide electrical and mechanical connection between the microelectronic part and the outside world [21]. Packaging of MEMS is much more complex than that for the IC due to the inherent complexities in structures and intended performances. Many MEMS products involve precision movement of solid components and need to interface with different outside environments, the latter being determined by their specific functions of biological, chemical, electromechanical, and optical nature. Therefore, MEMS packaging processes have to provide more functionalities including better mechanical protection, thermal management, hermetic sealing, complex electricity, and signal distribution [22].

A schematic illustration of a typical MEMS packaging is shown in **Figure 1**. Both the MEMS sensor die and the application specific integrated circuit (ASIC) are mounted onto a substrate using a die attach adhesive. The sensor die is covered by a MEMS cap in order to prevent any particles to ruin the sensitive part. Thereafter, they are wire bonded to acquire the electric connection and enclosed by the molding compound to provide protection from mechanical or environmentally induced damages [12].

Packaging, in particular, is an integral part of the MEMS design and plays a crucial role in the device stability. Package-induced stresses appear to be unavoidable in almost all MEMS components due to CTEs' (Coefficient of Thermal Expansion) mismatch of the packaging materials during the packaging process, especially in the die bonding and sealing process. The stresses existing in structures and interfaces form a stable equilibrium of micro-devices based on deformation compatibility conditions [23]. The formed equilibrium, however, is prone to be upset by the shift of material properties and/or structure expansion induced by the temperature load. The material aspects are always related to the packaging adhesive
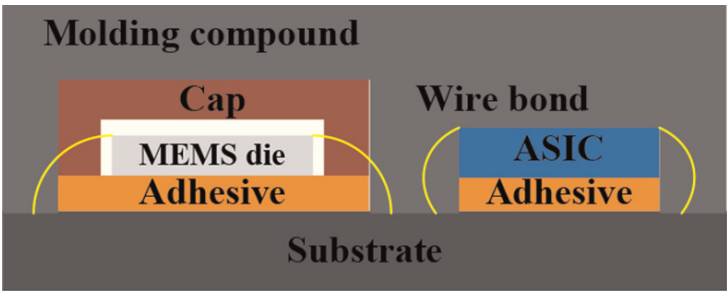

Figure 1.
A schematic illustration of typical MEMS packaging.

because silicon, glass, and ceramic exhibit an excellent stable property. This adhesive however, a polymer-based material, is often simply assumed to be linear elastic [24–26]. This assumption could give a relatively accurate evaluation of device performance in the low- and medium-precision application fields, but could not be used to predict the long-term stability or drift in areas requiring high precision without taking in consideration the viscoelasticity of polymers [27]. This chapter will deal with the stability regarding the viscoelasticity of packaging materials. With regard to the structure aspects, the main reliability issue is the thermal effects induced by the temperature change. The level of effects is attributed to the range of thermal mismatch and the structural layout. The former is unchangeable for a specific device because the structural materials are readily selected, while the latter, although of interest, lacks to attract further research, because researchers preferred a temperature compensation by external components than search for the underlying mechanism of thermal effects of devices. The current compensation technology can be categorized into active compensation and passive compensation.

1.1 Active compensation

Active compensation requires a temperature sensor to measure the device operating temperature, which is then fed back to a controller to keep the environment temperature constant. This is achieved by means of an algorithm and a thermometer, so as to control and compensate the output offset induced by temperature change.

The temperature control is the most widely applied technology regarding active compensation. However, the micro-oven may be regarded as a disadvantage of this technology, because it makes the device much bigger. In order to overcome this, Xu et al. [28] proposed a miniaturized and integrated heater that enables low power. Besides temperature control, modification of the performance is another broadly used compensation technology. For the MEMS sensor, its thermal drifts, such as thermal drift of bias (TDB) and thermal drift of scale factor (TDSF), are usually tested and recorded firstly. Then, when the MEMS sensor is in operation, the output is modified mathematically based on the recorded thermal drifts. For the MEMS resonator, the frequency modification by electrostatic stiffness is a frequently used technology [29]. In this technology, the temperature is fed back to control the operating voltage of the MEMS resonator and then change the electrostatic stiffness and consequently the frequency.

The position of the temperature sensor is critical for the compensation technology of the modification of the performance. In many MEMS devices, the temperature is integrated in the ASIC die, and the ASIC die is integrated with the MEMS die through the package. As such, the temperature sensors actually measure the temperature of the ASIC die. This, though, is error-prone regarding the temperature measurement of the MEMS die. In order to improve the temperature accuracy, several innovative technologies for temperature measuring have been proposed [30–32].

In order to compensate the thermal drift of frequency of MEMS resonator, Hopcroft et al. [33] extracted the temperature information from the variation of the quality factor. Kose et al. [34] reported a compensation method for a capacitive MEMS accelerometer by using a double-ended tuning fork resonator integrated with the accelerometer on the same die for measuring temperature. Du et al. [35] presented a real-time temperature compensation algorithm for a force-rebalanced MEMS capacitive accelerometer which relies on the linear relationship between the temperature and its dynamical resonant frequency.

1.2 Passive compensation

Active compensation is simpler and uncomplicated; however, it typically involves the additional circuitry and power consumption. On the contrary, the passive compensation does not need the additional circuitry and power consumption.

1.2.1 Passive compensation for TCEM

The current passive compensation technology for temperature coefficient of elastic modulus (TCEM) includes electrostatic stiffness modification, composite structure, and high doping. Melamud et al. [36] proposed a Si-SiO$_2$ composite resonator, as shown in **Figure 2a**. SiO$_2$ covers the surface of the silicon beam to form a composite resonator beam. Because TCEMs of silicon and SiO$_2$ are negative and positive, respectively, the Si-SiO$_2$ composite resonator can realize the passive compensation for the thermal drift of frequency. Liu et al. [37] also proposed an Al/SiO$_2$ composite MEMS resonator with the passive compensation ability for the thermal drift of frequency.

TCEM of single crystal silicon can also be compensated by high doping. A suggested mechanism is that heavy doping strains the crystal lattice and shifts the electronic energy bands, resulting in a flow of charge carriers to minimize the free energy, thereby changing the elastic properties [38]. Hajjam [39] reported a high phosphorus-doped silicon MEMS resonator with thermal drift of frequency down to 1.5 ppm/°C. Samarao [40] reported that MEMS resonator with high concentration
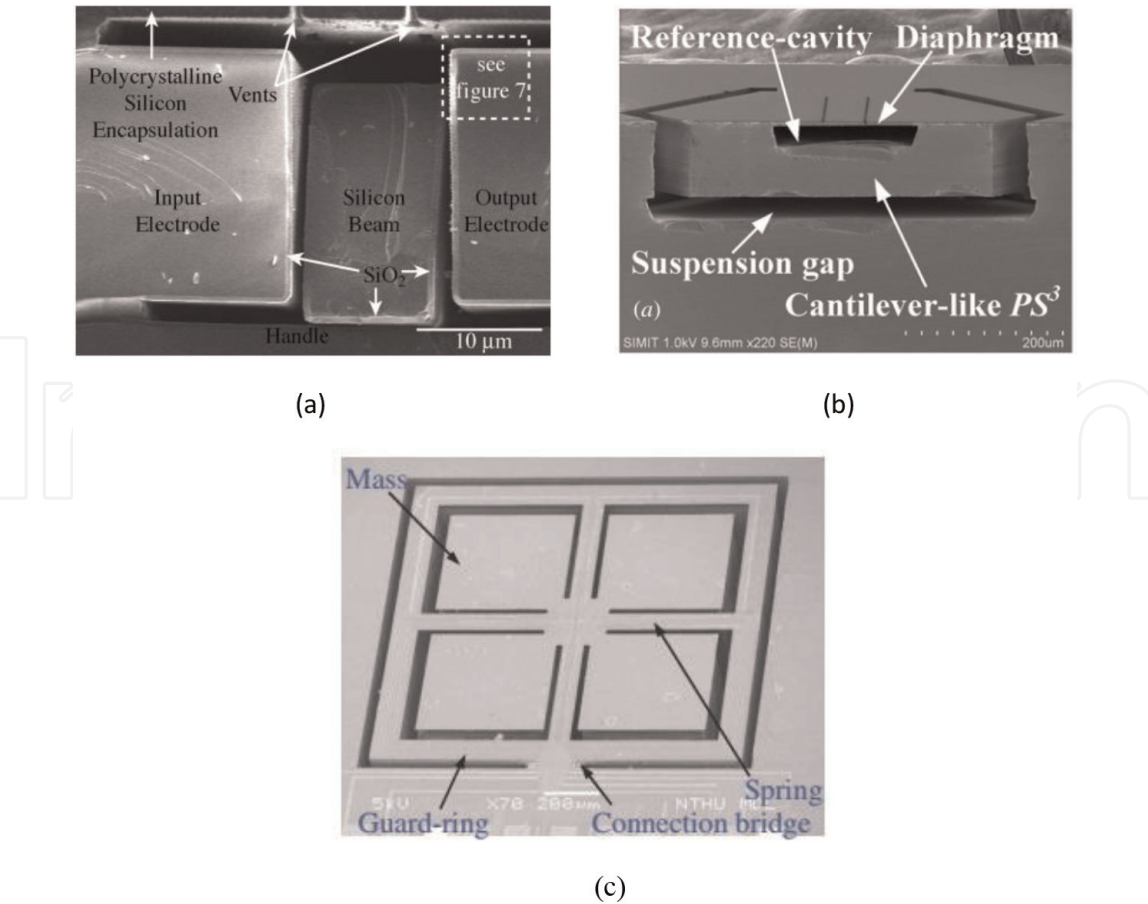

(a)

(b)

(c)

Figure 2.
MEMS devices with passive compensation, the ability of isolating the thermal stress. (a) Composite resonator [36], (b) pressure sensor isolating the thermal stress [43], and (c) three-axis piezo-resistive accelerometer pressure sensor isolating the thermal stress [44].

of boron doping and aluminum has thermal drifts of 1.5 and 2.7 ppm/°C, respectively.

The result of passive compensation depends on the precise structure design and is susceptible to fabrication error. As such, passive compensation generally cannot suppress the thermal drift fully. In several reports, active compensation and passive compensation are incorporated to suppress the thermal drift. For instance, Lee et al. [41] incorporate the electrostatic stiffness and Si-SiO$_2$ composite structure to compensate the thermal drift of the frequency of MEMS resonator. As such, 2.5 ppm drift of frequency over 90°C full scale is obtained.

1.2.2 Passive compensation for thermal stress/deformation

The improvement on structure design or package to suppress the thermal stress/deformation is an effective passive compensation technology for thermal stress/deformation.

The soft adhesive attaching, such as using rubber adhesive with an elastic modulus lower than 10M, is commonly employed to suppress thermal stress/deformation induced by the package [42]. Furthermore, the soft attaching area is also reduced to obtain lower thermal stress/deformation. Besides the passive compensation technology in packaging, improvement on structure design is also successfully employed to suppress thermal stress/deformation. Wang et al. [43] proposed a pressure sensor structure that can isolate stress, as shown in **Figure 2b**. They used cantilever beam to suspend the detection component of the pressure sensor, thereby isolating the influence of encapsulation effect on the sensor. Based on a floating ring, Hsieh et al. [44] suggested a three-axis piezo-resistive accelerometer with low thermal drift, as shown in **Figure 2c**.

1.2.3 Making the TCEM and thermal stress/deformation compensate each other

It is very promising to make the TCEM and thermal stress/deformation balance each other out. Hsu et al. [45] used thermal deformation to adjust the capacitance gap, so as to achieve the automatic adjustment of electrostatic stiffness and compensation for the variation of mechanical stiffness induced by temperature. Myers et al. [46] employed the thermal stress caused by the mismatch of CTE to compensate the frequency drift induced by TCEM. In this chapter, the thermal analysis is carried out in order to investigate the impacts of a structured layout of a sensing element on the drift over temperature of micro-accelerometers, and an optimized structure is proposed to improve the thermal stability.

2. Reliability analysis and experiments

2.1 Reliability regarding viscoelasticity

2.1.1 Polymer viscoelasticity

Viscoelasticity is a distinguishing characteristic of materials such as polymer. It exhibits both elastic and viscous behavior. The elasticity responding to stress is instantaneous, while the viscous response is time-dependent and varies with temperature. The viscoelastic behavior can be expressed with Hookean springs and Newtonian dashpot, which correspond to elastic and viscous properties, respectively. To measure the viscoelastic characteristics, stress relaxation or creep tests are often implemented. Stress relaxation of viscoelastic materials is commonly

described using a generalized Maxwell model, which is shown in **Figure 3**. It consists of a number of springs and dashpots connected in parallel, which represent elasticity and viscosity, respectively.

The Maxwell model can be described as a Prony series, which can be expressed with Eqs. (1) and (2) as below [47]:

$$E(t) = \frac{\sigma(t)}{\varepsilon_0} = E_\infty + \sum_{i=1}^{N} E_i \exp\left(-\frac{t}{\tau_i}\right) \tag{1}$$

$$\tau_i = \frac{\eta_i}{E_i} \tag{2}$$

where $E_{(t)}$ is the relaxation modulus; $\sigma_{(t)}$ is the stress; ε_0 is the imposed constant strain; E_∞ is the fully relaxed modulus; E_i and τ_i are referred to as a Prony pair; E_i and η_i are the elastic modulus and viscosity of Prony pair; τ_i is the relaxation time of ith Prony pair; N is the number of Prony pairs.

The relaxation data, for normalization, can be modeled by a master curve, which translates the curve segments at different temperatures to a reference temperature with logarithmic coordinates according to a time-temperature superposition [48]. The master curve can be fitted by a third-order polynomial function, such as

$$\log a_T(T) = C_1(T - T_0) + C_2(T - T_0)^2 + C_3(T - T_0)^3 \tag{3}$$

where a_T is the offset values at different temperatures (T); C_1, C_2, and C_3 are constants; and T_0 is the reference temperature.

Taking an epoxy die adhesive used in a MEMS capacitive accelerometer as an example, a series of stress-relaxation tests were performed using dynamic mechanical analysis [49]. The experimental temperature range was set from 25 to 125°C with an increment of 10°C and an increase rate of 5°C/min, and at each test point, 5 min was allowed for temperature stabilization, and 0.1% strain was applied on the adhesive specimen for 20 min, followed by a 10 min recovery. The test results are shown in **Figure 4**.

The shift distance of individual relaxation curve with reference temperature of 25°C was shown in **Figure 5**. Then the three coefficients of the polynomial function (Eq. (3)) were determined to be C_1 = 0.223439, C_2 = −0.00211, and C_3 = 5.31163 × 10^{-6}.

Subsequently the master curve can be acquired, and a Prony series having nine Prony pairs (Eq. (1)) was used to fit to the master curve, as shown in **Figure 6**. The coefficients of the Prony pairs are listed in **Table 1**, where E_0 is the instantaneous modulus when time is zero.
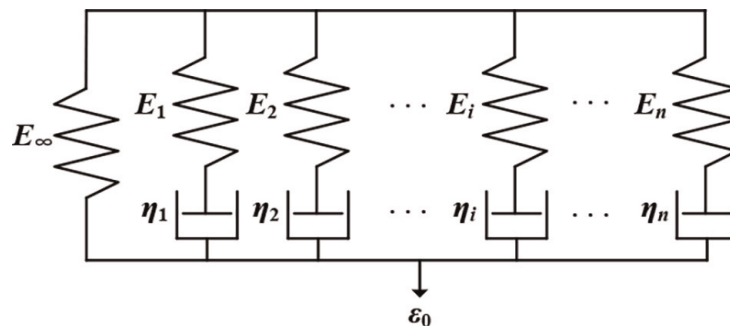

Figure 3.
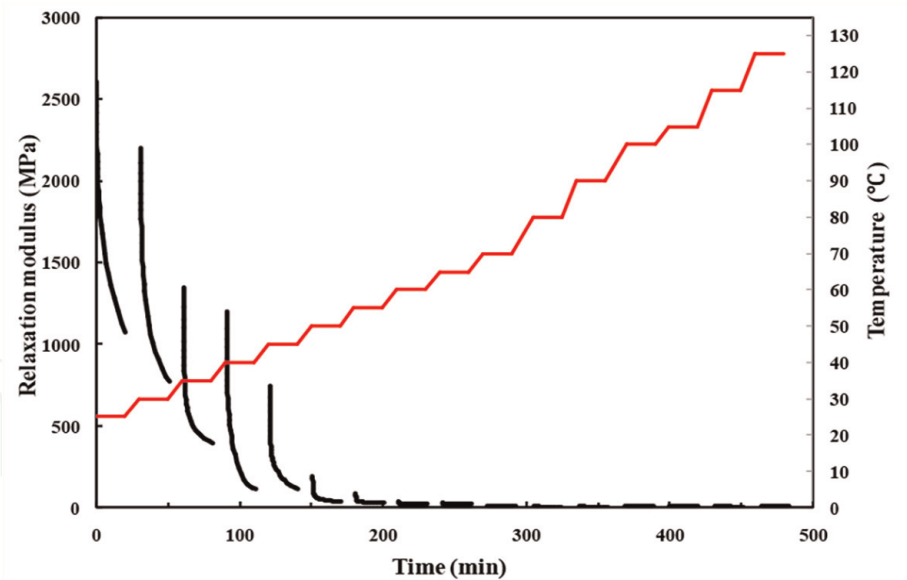*Generalized Maxwell model to describe the viscoelastic behavior.*

Figure 4.
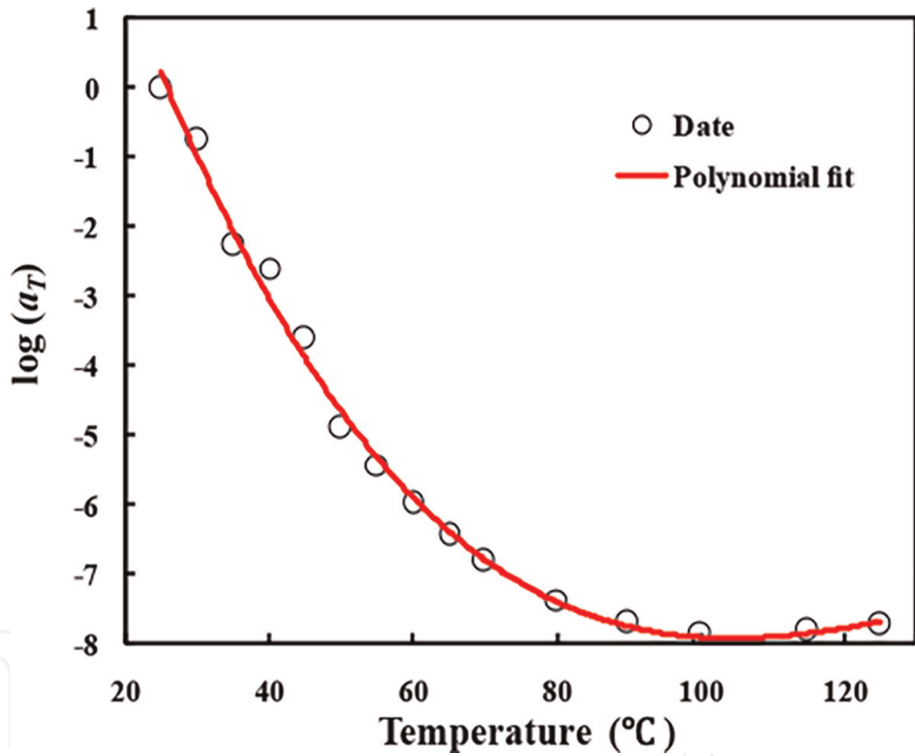*Stress-relaxation test results of an epoxy die attach adhesive.*

Figure 5.
Shift distance plot of individual relaxation curve with reference temperature of 25°C and polynomial fit.

2.1.2 Viscoelasticity-induced stability problem of MEMS

The viscoelasticity-related issue has become one of the most critical steps for assessing the packaging quality and output performance of highly precise MEMS sensors [50]. Applying the viscoelastic property to model the MEMS devices could yield a better agreement with the results observed in experiments than the previous elastic model [51]. The packaging stress in the MEMS was influenced not only by the temperature change but also by its change rate due to the time-dependent property of polymer adhesives [52]. Besides, the viscoelastic behavior influenced by moisture was recognized as the cause of the long-term stability of microsensors in storage [53].
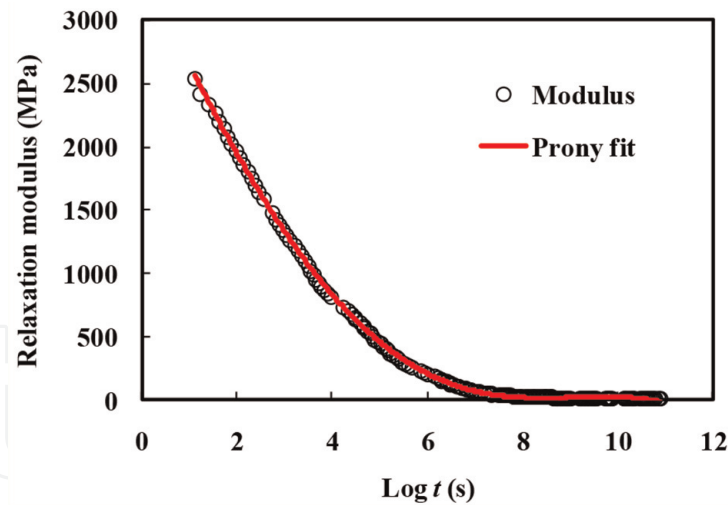
Figure 6.
Prony series fitted to master curve.

i	E_i/E_0	τ_i
1	0.08510	3041.87694
2	0.14589	981765.85865
3	0.22654	243.32699
4	0.11248	2083.25650
5	0.15906	48993.21024
6	0.21617	31.16988
7	0.03923	5052.23180
8	0.00025	6992.77554
9	0.00676	3321.33054

E_0 = 2744.76252 MPa.

Table 1.
Prony pairs of the die attach adhesive.

In the following, the output stability of a capacitive micro-accelerometer was investigated using both simulation and experimental methods. The simulation introduced the Prony series modulus into the whole finite element model (FEM) in Abaqus software to acquire the output of the micro-accelerometers over time and temperature. The thermal experiment was carried out in an incubator with an accurate temperature controller. The full loading history used in both simulation and the experiment is shown in **Figure 7**. The red-marked points represent the starting or ending points of a loading step. The bias and sensitivity of the accelerometers subjected to the thermal cycles are shown in **Figure 8**. The observed output drift in the simulation and the experiments indicates that the viscoelasticity of adhesive was the main cause of the deviation of zero offset and sensitivity. The underlying mechanism can be attributed to the time- and temperature-dependent stress and deformation states of the sensitive components of the micro-accelerometers.

It is evident that the output of the sensor after each thermal cycle will not change if the adhesive is assumed to be linear elastic.

The storage long-term drift of the accelerometer was also assessed by simulation and experimental methods based on the viscoelasticity of polymer adhesive. The residual stress formed in the curing process of the packaging would develop over time due to the internal strain changing with the relaxation of stress.
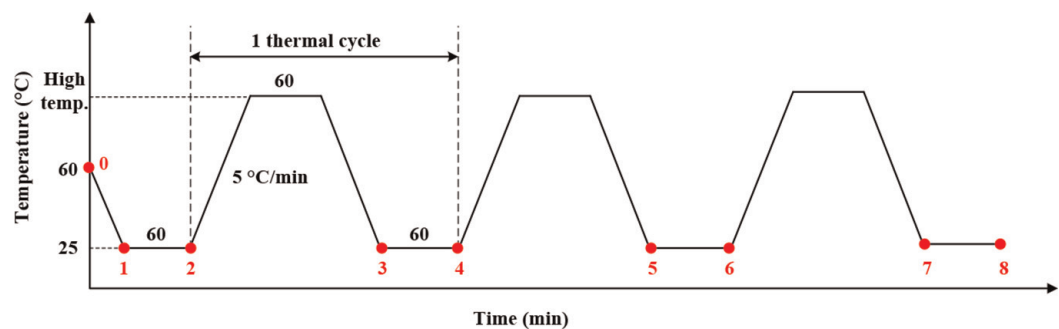
Figure 7.
Loading history for the analysis.

The temperature profile in the simulation started from 60 (curing temperature) to 25°C (room temperature), and then the sensor was kept at 25°C for 12 months. The variation of the bias of the sensor was shown in **Figure 9**. The bias decreased over time due to stress relaxation and declined by about 21 mg in 12 months. After the sensor was kept at 25°C for about 10 months, the bias reached a steady state (< 1 mg per month). The variation trend of the bias is generally consistent with the master curve of the relaxation modulus (**Figure 5**), which indicates that the package-induced stress will gradually be released because of adhesive viscoelastic characteristic in the long-term storage period.

2.2 Thermal drift of MEMS devices

The thermal drift of MEMS devices is related to its material, structure, interface circuit, and so on. The temperature coefficient of elastic modulus (TCEM) and the thermal stress/deformation are the factors studied mostly.

2.2.1 TCEM

Due to the excellent mechanical property, single crystal silicon is suitable for high-performance sensors, oscillators, actuators, etc. However, the elastic modulus of single crystal silicon is temperature dependent. Because the single crystal silicon is anisotropic, the temperature behavior of elasticity is more properly described by the temperature coefficients of the individual components of the elasticity tensor, Tc_{11}, Tc_{12}, etc., as shown in **Table 2**. In order to simplify the designing, the value of TCEM for typical axial loading situations is usually employed and equal to approximately -64 ppm/°C at room temperature [54].

The performance of MEMS devices is influenced by TCEM through the stiffness. In fact, the temperature coefficient of stiffness (TCS) is the sum of TCEM and CTE (coefficient of thermal expansion). CTE is 2.6 ppm/°C at room temperature and much smaller than TCEM. Therefore, TCS is mainly determined by TCEM. The effect of TCEM on performance is dependent on the principle of the MEMS device. If the MEMS device is oscillating at a fixed frequency for time reference, sensing or generating Coriolis force, its frequency has a thermal drift of TCS/2, because the frequency is related to the square root of stiffness. On the other hand, the thermal drift of the MEMS device, which the mechanical deformation is employed for sensing, such as the capacitive sensor, is equal to TCS, because the performance is related to the stiffness [55].

2.2.2 Thermal stress/deformation

Single crystal silicon expands with temperature and has a CTE of 2.6 ppm/°C at room temperature. The expansion induced by CTE can cause the variation of
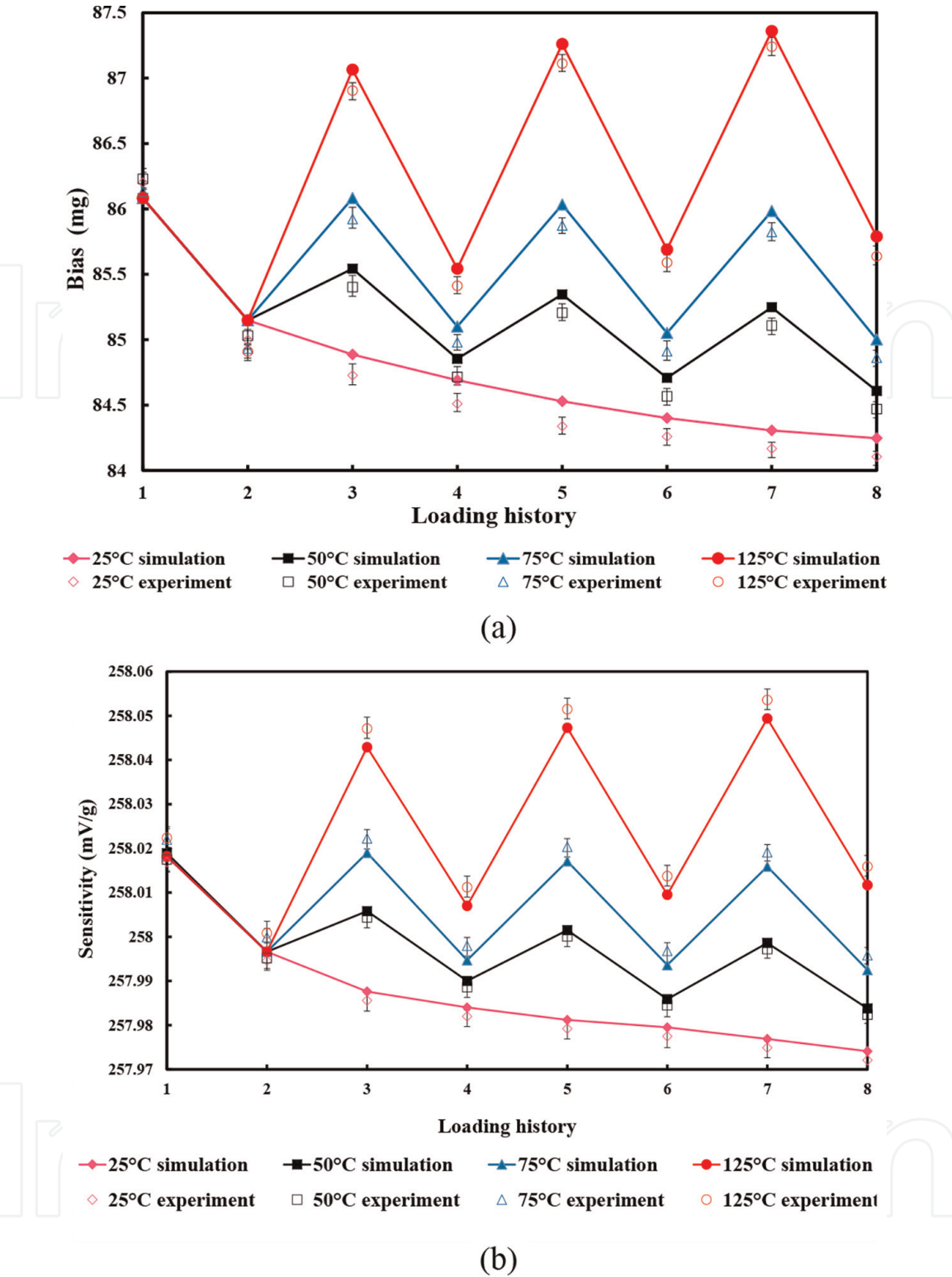
(a)

(b)

Figure 8.
Results comparison: (a) bias and (b) sensitivity.

geometric dimension, such as gap, width, and length, and consequently induce the performance drift of MEMS device. However, the performance drift induced by CTE is generally very small compared to that induced by CTE mismatch.

Besides the single crystal silicon, there often exist the layers made of other material in a MEMS die, such as glass, SiO_2, metal, and so on. The CTE of these materials is generally different from the single crystal silicon. Even for the borosilicate glass that has a CTE very close to the single crystal silicon, there still exists a CTE mismatch, as shown in **Figure 10**. In literature [57], research shows that the CTE difference between single crystal silicon and borosilicate glass induces bias
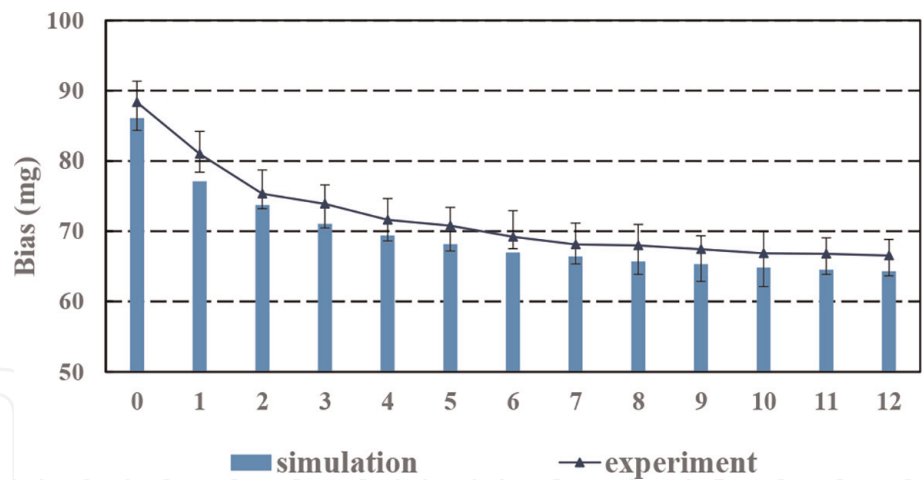
Figure 9.
The variation of the bias of the sensor in 12 months.

TCE	p-type (4 Ω cm, B)	n-type (0.05 Ω cm, P)	p-type (4 Ω cm, B)	n-type (0.05 Ω cm, P)
	First-order ($\times 10^{-6}$/K)		Second-order ($\times 10^{-6}$/K^2)	
TCE_{C11}	-73.25 ± 0.49	-74.87 ± 0.99	-49.26 ± 4.8	-45.14 ± 1.4
TCE_{C12}	-91.59 ± 1.5	-99.46 ± 3.5	-32.70 ± 10.1	-20.59 ± 11.0
TCE_{C44}	-60.14 ± 0.20	-57.96 ± 0.17	-51.28 ± 1.9	-53.95 ± 1.8

Table 2.
Temperature coefficients of the elastic constants given by Bourgeois et al. [56].
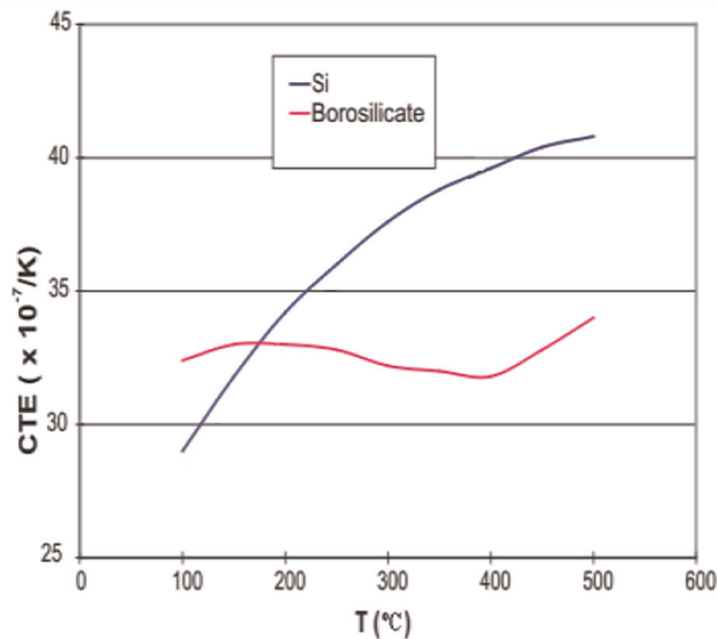

Figure 10.
CTE of silicon and borosilicate glass [61].

drift of MEMS accelerometer. Besides the CTE mismatch in MEMS die, another source of thermal stress/deformation is the CTE disagreement between the MEMS die and the package. The package material is in most cases ceramic, metal, and polymer, whose CTE values differ from the single crystal silicon. For instance, the CTE of a ceramic package is over twice as much as that of single crystal silicon [58]. In order to calculate the thermal stress/deformation, finite element method is
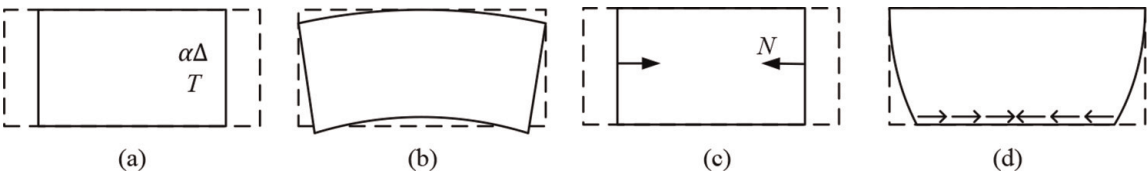
Figure 11.
Four components of the deformation in the die or substrate. (a) Longitudinal normal deformation induced by the thermal expansion, (b) longitudinal normal deformation induced by the shear stress, (c) transverse bending deformation, and (d) longitudinal shearing deformation.
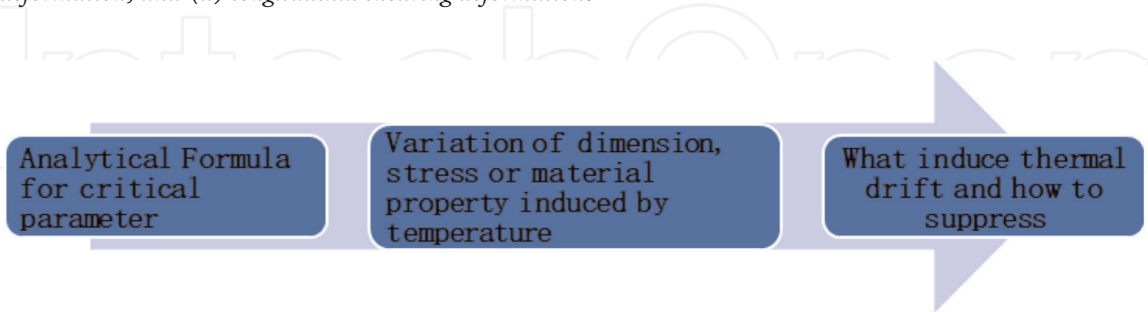

Figure 12.
Thermal drift procedure estimation.

widely employed. However, the finite element method generally generates a model with high degrees and is time-consuming. For the thermal stress/deformation induced by the package, the analytical model based on strength of material is also largely employed, while taking up less time. In the analytical model, the elastic foundation for the adhesive layer is generally employed [59], and the deformation inside the die or substrate is by and large divided into four components, which are shown in **Figure 10**. The four components can be described by the first-order or second-order beam theory [60] (**Figure 11**).

2.2.3 Means of estimating thermal drift

In this section, the procedure estimating the thermal drift is discussed, as shown in **Figure 12**. A case study about the thermal drift of a MEMS capacitive accelerometer is also presented.

The procedure estimating the thermal drift can be divided into three distinct steps:

1. Deriving analytical formulae for critical parameter(s)

This step forms the base of the latter two steps. Defining the precise critical parameter that needs to be derivated depends on application requirement. For instance, the drift of frequency is critical for the application of the MEMS resonator, so the analytical formula for frequency needs to be derived. The imperfection is important in obtaining analytical formulae for critical parameters, especially for the MEMS sensors employing the differential detecting principle. If the imperfection is not considered, such as the asymmetry induced by fabrication error, the bias of MEMS sensors nulls. As such, no result on the thermal drift of bias may be obtained.

2. Calculation of the variation of dimension, stress, or material property induced by temperature

It is critical to calculate the variation of dimension, stress, or material property induced by temperature for estimating the thermal drift. For the material property, its variation with temperature is induced by the temperature coefficient. However, for the dimension and stress, the variation generally needs to be calculated by finite

element analysis or other analytical methods. The imperfection is also important for the MEMS sensors employing the differential detecting principle. If the imperfection is not considered, the impact of the variation of dimension and stress is operating in common mode. As such, these variations cannot induce the variation of the bias for the MEMS sensors employing the differential detecting principle.

3. Discussion on the factors affecting the thermal drift and how to suppress the thermal drift

Based on the variation of dimension, stress, or material property induced by temperature, the thermal drift can be acquired by deriving the differential of the temperature. Then, the factors affecting thermal drift and how to suppress this will be discussed.

2.2.4 Case study

In the following, a MEMS capacitive accelerometer is employed to showcase the procedure estimating the thermal drift. The detection of the accelerometer is based on the open-loop differential capacitive principles, as shown in **Figure 13**. The acceleration force makes the proof mass move and is balanced by elastic force generated by folded beams. The moving proof mass changes the capacitances of the accelerometer. The detected variation amplitude of the capacitance difference between capacitors C_A and C_B via modulation and demodulation with preload AC voltage was used to generate the output voltage:

$$V_{out} = G\frac{C_A - C_B}{C_A + C_B} \tag{4}$$

where G is the gain that depends on the circuit parameters.

Based on the detecting principle and the dimension shown in **Figure 13b**, the bias and scale factor are expressed as
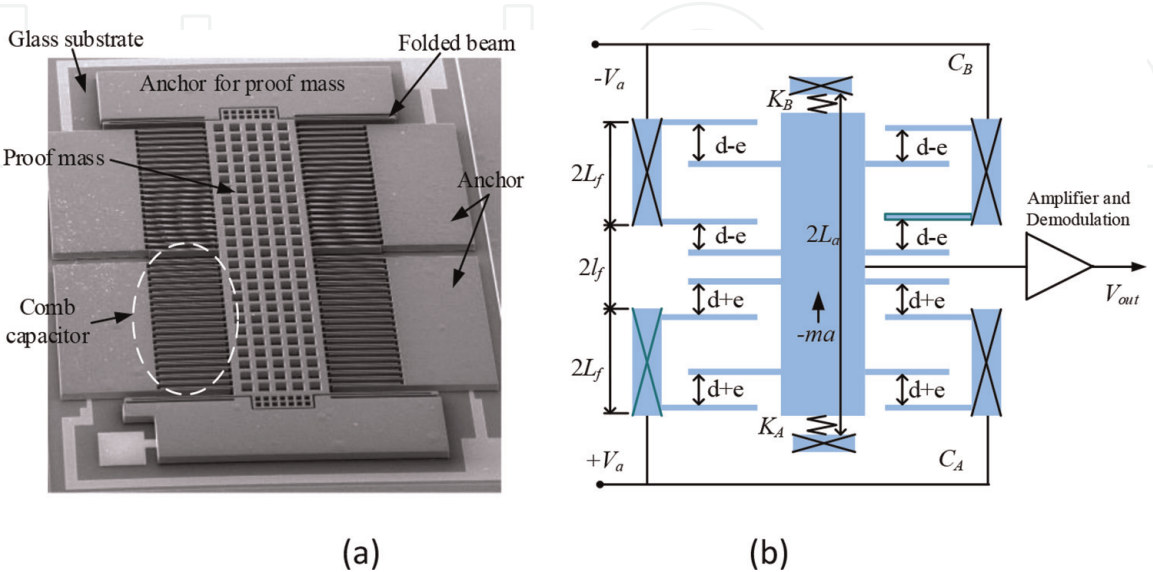
$$B = -\frac{K_T e}{m} \tag{5}$$

(a)   (b)

Figure 13.
MEMS capacitive accelerometer employed as case study. (a) SEM picture and (b) open-loop differential capacitive principle. ±Va is preload AC voltage. CA and CB represent capacitors on the bottom and top sides, respectively.

$$k_1 = G\frac{m}{dK_T} \tag{6}$$

where B and k_1 represent the bias and scale factor, respectively; K_T is the total stiffness of the folded beams; m is the total mass of proof mass and moving fingers; e represents the asymmetry of capacitive gap induced by the fabrication error; d is the capacitive gap.

From the equation of bias, it can be seen that if the asymmetry of capacitive gap is not considered, then the bias nulls. In equations of bias and scale factor, the parameters varying with temperature include K_T, e, and d. Variation of the stiffness is induced by TCEM and CTE [7]:

$$TCS = \frac{1}{K_T}\frac{dK_T}{dT} = \alpha_E + \alpha_s \tag{7}$$

The variations of e and d are calculated by analytical method [44]:

$$\Delta e = \frac{K_A - K_B}{K_A + K_B}(\alpha_s - \alpha_{eq})\Delta T L_a \tag{8}$$

$$\Delta d = (d\alpha_s + (l_f + L_f)(\alpha_{eq} - \alpha_s))\Delta T \tag{9}$$

where L_a expresses the distance from the anchor to the midline; L_f denotes the half length of an anchor for fixed fingers; l_f defines the locations of first fixed finger, as shown in **Figure 13b**; α_s indicates the CTE of silicon; α_{eq} is called as equivalent CTE describing the thermal deformation of the top surface of the substrate and calculated by the analytical model for the MEMS die attaching proposed in literature; K_A and K_B stand for the spring stiffness connecting proof mass.

Deriving the differential of the bias to the temperature, the TDB is expressed as

$$TDB = \frac{\Delta B}{\Delta T} = -\frac{K_T \Delta e}{m\Delta T} = \frac{K_A - K_B}{m}(\alpha_{eq} - \alpha_s)L_a \tag{10}$$

Deriving the differential of the scale factor to the temperature, the thermal drift of scale factor (TDSF) is expressed as

$$TDSF = \frac{\Delta k_1}{k_1|_{\Delta T=0}\Delta T} = TCS - \left(\alpha_s + \frac{(l_f + L_f)(\alpha_{eq} - \alpha_s)}{d}\right) \tag{11}$$

Due to the asymmetry induced by the fabrication error, K_A and K_B are different from each other, and TDB is proportional to the difference between K_A and K_B. Therefore, the consideration on the imperfection is very important for discussing the thermal drift.

Based on the discussion on TDB and TDSF, the factors affecting thermal drift and method suppressing the thermal drift can be obtained:

1. The model shows that TDB is only caused by thermal deformation, while TDSF consists of two parts caused by stiffness temperature dependence and thermal deformation, respectively. The two parts of TDSF are positive and negative, respectively. However, the second part has a greater absolute value.

2. The first part of TDSF can be reduced by high doping. TDB and the second part of TDSF can be both reduced by soft adhesive die attaching or increasing substrate thickness.
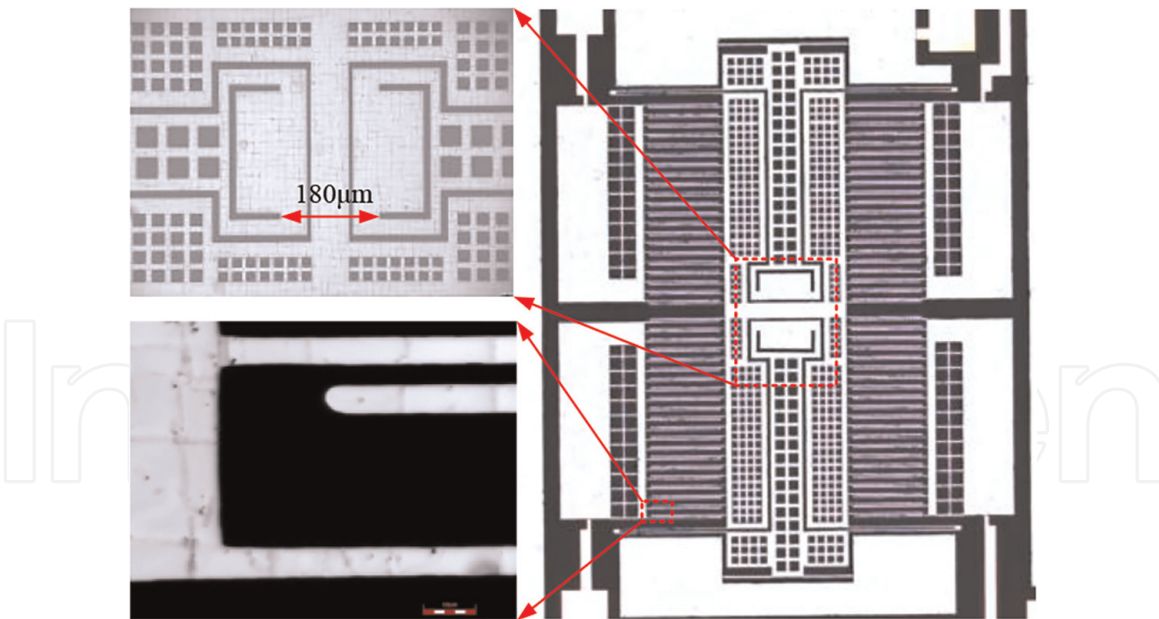
Figure 14.
Accelerometer with optimization for TDSF.

3. In silicon structure, TDB can be reduced by middle-locating anchors for moving electrodes in sensitive direction or decreasing the stiffness asymmetry of springs, while the second part of TDSF can be reduced by middle-locating anchors for fixed electrodes in sensitive direction.

The TDSF of the MEMS capacitive accelerometer can both be induced by the TCEM and the thermal deformation, so the structure of the accelerometer is optimized to make the TCEM and thermal deformation compensate each other, as shown in **Figure 14** [62]. As such, TDSF is suppressed significantly.

3. Conclusions

MEMS devices are an integrated system involving aspects of mechanics, electronics, materials, physics, and chemistry while interacting with the environment. Therefore, their reliability exhibits a great diversity of modes and mechanisms. This is a field open for further research, as it covers a vast area. However, one practical way is to conclude a few failure phenomena of a specific device for providing a guideline to study the similar behaviors appearing in other devices. This chapter only focused on the reliability problem occurring in the micro-accelerometers in storage and the thermal environment. These two factors pose the significant importance on the development of high-end microsensors for high-precise applications. The long-term stability induced by the viscoelasticity of packaging materials was first mentioned in this work to explain the performance shift after a long period of storage. The thermal effects formed by temperature change and structural layout were studied in depth and showed that the drift over temperature may be eliminated by a well-designed structure rather than perfect materials with zero CTE. It is the authors' view that this area should be further researched so as to bridge the diversity of micro-devices and develop standards.

Acknowledgements

Conflict of interest

The authors declare no conflict of interest.

Thanks

The authors would like to thank Prof. Xiaoping He, Prof. Lianming Du, and Prof. Zhigui Shi for their assistance in designing the circuit, setting up the experiment, and fabricating the sensors.

Author details

Wu Zhou[1*], Jiangbo He[2], Peng Peng[3], Lili Chen[3] and Kaicong Cao[1]

1 School of Mechanical and Electrical Engineering, University of Electronic Science and Technology of China, Chengdu, China

2 School of Mechanical Engineering, Xihua University, Chengdu, China

3 School of Mechanical Engineering, Chengdu Technological University, Chengdu, China

*Address all correspondence to: zhouwu916@uestc.edu.cn

IntechOpen

References

[1] Müller-Fiedler R, Wagner U, Bernhard W. Reliability of MEMS—A methodical approach. Microelectronics and Reliability. 2002;**42**(9–11): 1771-1776. DOI: 10.1016/S0026-2714 (02)00229-9

[2] Van Spengen WM. MEMS reliability from a failure mechanisms perspective. Microelectronics and Reliability. 2003; **43**(7):1049-1060. DOI: 10.1016/ S0026-2714(03)00119-7

[3] Van Spengen WM, Puers R, De Wolf I. The prediction of stiction failures in MEMS. IEEE Transactions on Device and Materials Reliability. 2003;**3**(4): 167-172. DOI: 10.1109/ TDMR.2003.820295

[4] Tanner DM. MEMS reliability: Where are we now? Microelectronics and Reliability. 2009;**49**(9–11):937-940. DOI: 10.1016/j.microrel.2009.06.014

[5] Fonseca DJ, Sequera M. On MEMS reliability and failure mechanisms. International Journal of Quality, Statistics, and Reliability. 2011;**2011**:7. Article ID 820243. DOI: 10.1155/2011/ 820243

[6] Huang Y, Vasan ASS, Doraiswami R, Osterman M, Pecht M. MEMS reliability review. IEEE Transactions on Device and Materials Reliability. 2012;**12**(2): 482-493. DOI: 10.1109/ TDMR.2012.2191291

[7] He J, Xie J, He X, Du L, Zhou W. Analytical study and compensation for temperature drifts of a bulk silicon MEMS capacitive accelerometer. Sensors and Actuators, A: Physical. 2016;**239**:174-184. DOI: 10.1016/j. sna.2016.01.026

[8] Peng P, Zhou W, Yu H, Peng B, Qu H, He X. Investigation of the thermal drift of MEMS capacitive accelerometers induced by the overflow of die attachment adhesive. IEEE Transactions on Components, Packaging and Manufacturing Technology. 2016;**6**(5):822-830. DOI: 10.1109/TCPMT.2016.2521934

[9] Kahn H, Heuer AH, Jacobs SJ. Materials issues in MEMS. Materials Today. 1999;**2**(2):3-7. DOI: 10.1016/ S1369-7021(99)80002-9

[10] Van Driel WD, Yang DG, Yuan CA, Van Kleef M, Zhang GQ. Mechanical reliability challenges for MEMS packages: Capping. Microelectronics and Reliability. 2007;**47**(9–11): 1823-1826. DOI: 10.1016/j. microrel.2007.07.033

[11] Sundaram S, Tormen M, Timotijevic B, Lockhart R, Overstolz T, Stanley RP, et al. Vibration and shock reliability of MEMS: Modeling and experimental validation. Journal of Micromechanics and Microengineering. 2011;**21**(4):045022. DOI: 10.1088/0960-1317/21/4/045022

[12] Tilmans HAC, De Coster J, Helin P, Cherman V, Jourdain A, Demoor P, et al. MEMS packaging and reliability: An undividable couple. Microelectronics and Reliability. 2012;**52**(9–10): 2228-2234. DOI: 10.1016/j.microrel. 2012.06.029

[13] Zhang W-M, Yan H, Peng Z-K, Meng G. Electrostatic pull-in instability in MEMS/NEMS: A review. Sensors and Actuators, A: Physical. 2014;**214**: 187-218. DOI: 10.1016/j.sna.2014.04.025

[14] Li J, Broas M, Makkonen J, Mattila TT. Shock impact reliability and failure analysis of a three-axis MEMS gyroscope. Journal of Microelectromechanical Systems. 2014;**23**(2):347-355. DOI: 10.1109/JMEMS.2013.2273802

[15] DelRio FW, Cook RF, Boyce BL. Fracture strength of micro- and

nano-scale silicon components. Applied Physics Reviews. 2015;**2**(2):021303. DOI: 10.1063/1.4919540

[16] Yu L-X, Qin L, Bao A-D. Reliability prediction for MEMS accelerometer under random vibration testing. Journal of Applied Science and Engineering. 2015;**18**(1):41-46. DOI: 10.6180/jase.2015.18.1.06

[17] Wang J, Zeng S, Silberschmidt VV, Guo J. Multiphysics modeling approach for micro electro-thermo-mechanical actuator: Failure mechanisms coupled analysis. Microelectronics and Reliability. 2015;**55**(5):771-782. DOI: 10.1016/j.microrel.2015.02.012

[18] Iannacci J. Reliability of MEMS: A perspective on failure mechanisms, improvement solutions and best practices at development level. Displays. 2015;**37**:62-71. DOI: 10.1016/j.displa.2014.08.003

[19] Shoaib M, Hamid NH, Malik A, Ali NBZ. A review on key issues and challenges in devices level MEMS testing. Journal of Sensors. 2016;**2016**: 1-14. DOI: 10.1155/2016/1639805

[20] Tavassolian N, Koutsoureli M, Papaioannou G, Papapolymerou J. Optimization of dielectric material stoichiometry for high-reliability capacitive MEMS switches. IEEE Microwave and Wireless Components Letters. 2016;**26**(3):174-176. DOI: 10.1109/LMWC.2016.2524596

[21] Cheng YT, Lin L. MEMS Packaging and Thermal Issues in Reliability. Berlin Heidelberg: Springer. 2004. p. 1112. DOI: 10.1007/3-540-29838-X_37

[22] Hsu TR. Reliability in MEMS packaging. In: Proceedings of the IEEE International Conference on Reliability Physics (ICRP'06); 26–30 March 2006; San Jose, CA: IEEE; 2006. pp. 398-402

[23] Ther JBN, Larsen A, Liverød B, et al. Measurement of package-induced stress and thermal zero shift in transfer molded silicon piezoresistive pressure sensors. Journal of Micromechanics and Microengineering. 1998;**8**(2):168-171. DOI: 10.1088/0960-1317/8/2/032

[24] Walwadkar SS, Cho J. Evaluation of die stress in MEMS packaging: Experimental and theoretical approaches. IEEE Transactions on Components and Packaging Technologies. 2006;**29**(4):735-742. DOI: 10.1109/TCAPT.2006.885931

[25] Chuang CH, Lee SL. The influence of adhesive materials on chip-on-board packing of MEMS microphone. Microsystem Technologies. 2012;**18**(11): 1931-1940. DOI: 10.1007/s00542-012-1575-0

[26] Peng P, Zhou W, Yu H, et al. Investigation of the thermal drift of MEMS capacitive accelerometers induced by the overflow of die attachment adhesive. IEEE Transactions on Components, Packaging and Manufacturing Technology. 2017;**6**(5): 822-830. DOI: 10.1109/TCPMT.2016.2521934

[27] Obaid N, Kortschot MT, Sain M. Understanding the stress relaxation behavior of polymers reinforced with short elastic fibers. Materials. 2017; **10**(5):472-486. DOI: 10.3390/ma10050472

[28] Xu C, Segovia J, Kim HJ, et al. Temperature-stable piezoelectric MEMS resonators using integrated ovens and simple resistive feedback circuits. Journal of Microelectromechanical Systems. 2016;**2016**:1-9. DOI: 10.1109/JMEMS.2016.2626920

[29] Ho GK, Sundaresan K, Pourkamali S, et al. Micromechanical IBARs: Tunable high-Q resonators for temperature-compensated reference oscillators. Journal of

Microelectromechanical Systems. 2010;
19(3):503-515. DOI: 10.1109/
JMEMS.2010.2044866

[30] Hopcroft MA, Agarwal M, Park KK, et al. Temperature compensation of a MEMS resonator using quality factor as a thermometer. In: Proceedings of the 19th IEEE International Conference on Micro Electro Mechanical Systems; 22–26 Jan. 2006; Istanbul, Turkey, Turkey: IEEE; 2006. DOI: 10.1109/ MEMSYS.2006.1627776

[31] Salvia JC, Melamud R, Chandorkar SA, et al. Real-time temperature compensation of MEMS oscillators using an integrated micro-oven and a phase-locked loop. Journal of Microelectromechanical Systems. 2010; **19**(1):192-201. DOI: 10.1109/ JMEMS.2009.2035932

[32] Kim B, Hopcroft MA, Candler RN, et al. Temperature dependence of quality factor in MEMS resonators. Journal of Microelectromechanical Systems. 2008;**17**(3):755-766. DOI: 10.1109/JMEMS.2008.924253

[33] Hopcroft MA, Kim B, Chandorkar S, et al. Using the temperature dependence of resonator quality factor as a thermometer. Applied Physics Letters. 2007;**91**(1):440. DOI: 10.1063/1.2753758

[34] Kose T, Azgin K, Akin T. Temperature compensation of a capacitive MEMS accelerometer by using a MEMS oscillator. In: IEEE International Symposium on Inertial Sensors & Systems. 2016. DOI: 10.1109/ ISISS.2016.7435538

[35] Du J, Guo Y, Lin Y, et al. A real-time temperature compensation algorithm for a force-rebalanced MEMS capacitive accelerometer based on resonant frequency. In: IEEE International Conference on Nano/micro Engineered & Molecular Systems; IEEE; 2017. DOI: 10.1109/NEMS.2017.8017009

[36] Melamud R, Chandorkar SA, Kim B, et al. Temperature-insensitive composite micromechanical resonators. Journal of Microelectromechanical Systems. 2009;**18**(6):1409-1419. DOI: 10.1109/JMEMS.2009.2030074

[37] Liu YC. Temperature-compensated CMOS-MEMS oxide resonators. Journal of Microelectromechanical Systems. 2013;**22**(5):1054-1065. DOI: 10.1109/ JMEMS.2013.2263091

[38] Ng EJ, Hong VA, Yang Y, et al. Temperature dependence of the elastic constants of doped silicon. Journal of Microelectromechanical Systems. 2015; **24**(3):730-741. DOI: 10.1109/ JMEMS.2014.2347205

[39] Hajjam A, Logan A, Pourkamali S. Doping-induced temperature compensation of thermally actuated high-frequency silicon micromechanical resonators. Journal of Microelectromechanical Systems. 2012; **21**(3):681-687. DOI: 10.1109/ jmems.2012.2185217

[40] Samarao AK, Ayazi F. Temperature compensation of silicon resonators via degenerate doping. IEEE Transactions on Electron Devices. 2012;**59**(1):87-93. DOI: 10.1109/ted.2011.2172613

[41] Lee H, Kim B, Melamud R, et al. Influence of the temperature dependent nonlinearities on the performance of micromechanical resonators. Applied Physics Letters. 2011;**99**(19):194102. DOI: 10.1063/1.3660235

[42] Zwahlen P, Nguyen A, Dong Y, et al. Navigation grade MEMS accelerometer. IEEE International Conference on MicroElectro Mechanical Systems; Hong Kong, China; 2010. pp. 631-634. DOI: 10.1109/ MEMSYS.2010.5442327

[43] Wang J, Li X. Package-friendly piezoresistive pressure sensors with on-chip integrated packaging-stress-

suppressed suspension (PS3) technology. Journal of Micromechanics and Microengineering. 2013;**23**(4): 045027. DOI: 10.1088/0960-1317/23/4/045027

[44] Hsieh HS, Chang HC, Hu CF, et al. A novel stress isolation guard-ring design for the improvement of a three-axis piezoresistive accelerometer. Journal of Micromechanics and Microengineering. 2011;**21**(10):105006. DOI: 10.1088/0960-1317/21/10/105006

[45] Hsu WT, Nguyen TC. Stiffness compensated temperature in-sensitive micromechanical resonators. In: IEEE International Conference on Micro Electro Mechanical Systems; Las Vegas, USA; 2002. pp. 731-734. DOI: 10.1109/MEMSYS.2002.984374

[46] Myers DR, Azevedo RG, Chen L, et al. Passive substrate temperature compensation of doubly anchored double-ended tuning forks. Journal of Microelectromechanical Systems. 2012; **21**(6):1321-1328. DOI: 10.1109/JMEMS.2012.2205903

[47] Kim YK, White SR. Stress relaxation behavior of 3501-6 epoxy resin during cure. Polymer Engineering and Science. 2010;**36**(23):2852-2862. DOI: 10.1002/pen.10686

[48] Hu M, Xia Y, Daeffler CS, et al. The linear rheological responses of wedge-type polymers. Journal of Polymer Science Part B: Polymer Physics. 2015; **53**:899-906. DOI: 10.1002/polb.23716

[49] Zhou W, Peng P, Yu H, et al. Material viscoelasticity-induced drift of micro-accelerometers. Materials. 2017; **10**(9):1077-1087. DOI: 10.3390/ma10091077

[50] Zhang X, Park S, Judy MW. Accurate assessment of packaging stress effects on MEMS sensors by measurement and sensor-package interaction simulations. Journal of Microelectromechanical Systems. 2007; **16**(3):639-649. DOI: 10.1109/JMEMS.2007.897088

[51] Krondorfer RH, Kim YK. Packaging effect on MEMS pressure sensor performance. IEEE Transactions on Components and Packaging Technologies. 2007;**30**(2):285-293. DOI: 10.1109/TCAPT.2007.898360

[52] Park S, Liu D, Kim Y, et al. Stress evolution in an encapsulated MEMS package due to viscoelasticity of packaging materials. In: Proceedings of the IEEE Electronic Components and Technology Conference (ECTC'12); 29 May–1 June 2012; San Jose, CA: IEEE; 2012. pp. 70-75

[53] Kim Y, Liu D, Lee H, Liu R, et al. Investigation of stress in MEMS sensor device due to hygroscopic and viscoelastic behavior of molding compound. IEEE Transactions on Components, Packaging and Manufacturing Technology. 2015;**5**(7): 945-955. DOI: 10.1109/tcpmt.2015.2442751

[54] Hopcroft MA, Nix WD, Kenny TW. What is the Young's modulus of silicon? Journal of Microelectro-mechanical Systems. 2010;**19**(2):229-238. DOI: 10.1109/JMEMS.2009.2039697

[55] Dong Y, Zwahlen P, Nguyen AM, et al. Ultra-high precision MEMS accelerometer. In: Proceedings of 2011 16th International Solid-State Sensors, Actuators and Microsystems Conference; 5–9 June 2011; Beijing, China: IEEE; 2011. DOI: 10.1109/TRANSDUCERS.2011.5969218

[56] Bourgeois C, Steinsland E, Blanc N, et al. Design of resonators for the determination of the temperature coefficients of elastic constants of monocrystalline silicon. IEEE International Frequency Control Symposium; IEEE; 1997. DOI: 10.1109/FREQ.1997.639192

[57] Dai G, Li M, He X, et al. Thermal drift analysis using a multiphysics model of bulk silicon MEMS capacitive accelerometer. Sensors and Actuators, A: Physical. 2011;**172**(2):369-378. DOI: 10.1016/j.sna.2011.09.016

[58] Erba A, Maul J, Demichelis R, et al. Assessing thermochemical properties of materials through ab *initio* quantum-mechanical methods: The case of α-Al_2O_3. Physical Chemistry Chemical Physics. 2015;**17**(17):11670-11677. DOI: 10.1039/C5CP01537E

[59] Wang J, Zeng S. Thermal stresses analysis in adhesive/solder bonded bimaterial assemblies. Journal of Applied Physics. 2008;**104**(11):113508. DOI: 10.1063/1.3021357

[60] He J, Zhou W, He X, et al. Analytical model for adhesive die-attaching subjected to thermal loads using second-order beam theory. International Journal of Adhesion and Adhesives. 2018;**82**:282-289. DOI: 10.1016/j.ijadhadh.2018.01.016

[61] SD-2—Glass Substrate for Silicon Sensors. Available from: http://www.hoyaoptics.com/pdf/silicon_sensor.pdf

[62] He J, Zhou W, Yu H, et al. Structural designing of a MEMS capacitive accelerometer for low temperature coefficient and high linearity. Sensors. 2018;**18**(2):643. DOI: 10.3390/s18020643